16th Australasian Fluid Mechanics Conference
Crown Plaza, Gold Coast, Australia
2-7 December 2007

CFD designed experiments for shock wave/boundary layer interactions in hypersonic ducted flows

A. G. Dann and R. G. Morgan

Centre for Hypersonics
Division of Mechanical Engineering
University of Queensland, Brisbane, Qld, 4072 AUSTRALIA

Abstract

The successful operation of scramjet combustors requires compression of hypersonic viscous ducted flows and avoidance of separation effects which may preclude steady flow. Separation effects in scramjet inlets and combustors can be caused by shock wave/boundary layer interactions. The hypersonic turbulent flow experiments needed are inherently difficult to design because of the high sensitivity of the macroscopic flow parameters which cause the turbulent flow processes. Hence computational fluid dynamics (CFD) is a useful tool for the design and characterisation of models in hypersonic flows before model construction. One of the greatest challenges however is to ensure that the flow is being modeled accurately. In this paper, a commercial code has been used to model an experiment performed in a small reflected shock tunnel using a Mach 8.65 condition. The research being carried out in this facility is concerned with separation due to incident shock wave/turbulent boundary interactions in hypersonic ducted flows. The model is designed to produce two conical shocks which interact with a turbulent boundary layer and it is instrumented with pressure transducers and thin film heat transfer gauges. The measurements have allowed graphical representation of unseparated static wall pressure and heat flux prior to and after each wall interaction. The results of the simulations are in excellent agreement with the experimental data. The code has been applied to identify parameter boundaries in the design of a model of similar scale that will produce separated flow.

Introduction

For high speed air-breathing engines, knowledge of the point at which boundary layer separation occurs limits the design parameters. Shock wave/turbulent boundary layer interactions are a common occurrence in supersonic flows with almost any flow deflection accompanied by shock formation. Incident shock interactions occur when the shock that impinges on the boundary layer is generated by an external source. These allow for the study of the interaction of bulk flow compression without the added effects of streamline curvature and hence they have been used for the experimental work in this paper. They are particularly important for scramjet studies which involve ducted flows where there is a requirement to add as much heat and pressure as possible. Unfortunately analytical means of modeling separated flow are not advanced. CFD codes however have progressed significantly to the point where several commercially available codes are capable of simulating hypersonic flows in reasonable time frames. When dealing with separated flows it is important to ensure the use of time accurate codes to capture upstream influences which is not possible with time marching codes. Turbulence models still need to be employed to approximate turbulent effects and these are most probably the cause of a large proportion of inaccuracies. Choice of the most appropriate turbulence model is therefore very important. Two-equation models are far more accurate when predicting boundary layer separation[1] however for unseparated flows simple algebraic models will often suffice.

Experimental Program

Facility

The experimental data for the following work has been obtained from T^2[2], a small free-piston reflected shock tunnel at the University of Queensland. The experimental results have been formulated from the one condition with stagnation conditions as shown in Table 1. The nozzle exit conditions, also presented in Table 1, were calculated using an equilibrium chemistry isentropic process from the stagnation results. These are based on the measured stagnation pressure, and the nozzle exit static and pitot pressures. The estimated Reynolds number is $7.5 \times 10^6/m$ which produces a turbulent boundary layer in the experimental model.

Table 1: Experimental stagnation and nozzle exit conditions

Stagnation Conditions		Nozzle Exit Conditions	
Stagnation pressure	$30.7MPa$	Density	$0.08kg/m^3$
Stagnation Temperature	$1310K$	Static pressure	$2.1kPa$
Incident Shock Speed	$1100m/s$	Pitot pressure	$200kPa$
		Velocity	$1700m/s$
		Mach no.	8.65

Experimental Model

Scramjet combustor flows are characterised by a complex combination of multiple shock and expansion wave systems originating from the intake compression and from heat release due to combustion. The traversing of these shocks through boundary layers limits the pressure rise which can be sustained without separation; which in turn limits the propulsive efficiency. In order to study this process from a fundamental point of view, a model was designed to create two sets of shock-expansion pairs which could traverse the boundary layer at preset distances.

The T^2 experiments involve an instrumented aluminium circular duct of inner diameter 38mm and length 420mm. The duct was instrumented longitudinally with eight PCB pressure transducers and six quartz thin-film heat transfer gauges. The model (Fig. 1) incorporates an inlet with a conically shaped cowl (not shown), and a shock generator incorporating two cones of 15° semivertex angles. The generator was moved incrementally rearward using the same condition at each shot in order to provide more data points and hence greater resolution. At the point of shock wave/boundary layer interaction the maximum change in boundary layer thickness by utilising this procedure is approximately ±5% which is of second significance when compared to the axial gradients being measured. The duct is sufficiently long so as to allow development of a turbulent boundary

layer that will thereby interact with the conical shocks created from the cones. The existence of a turbulent boundary layer was verified by comparison of experimental heat transfer data with laminar and turbulent correlations[3].

In order to avoid unwanted shock and expansion wave effects the model has been designed so that the first reflected shock is swallowed by an inner cylinder and removed from the area of interest. The second shock generator is able to be moved forward or rearward to adjust the second shock wave/boundary layer interaction position.

Data was recorded for three model configurations as shown in Fig. 1. The first configuration was to confirm that the pressure and heat flux peaks corresponded to the generation of shocks by the cones and not other features of the model i.e. the second cone was positioned far downstream, the second was based on results of an early viscous CFD simulation that showed separation after the second cone interaction, and the third was with the second cone as far forward as possible and still allowing the first reflected shock to be swallowed.
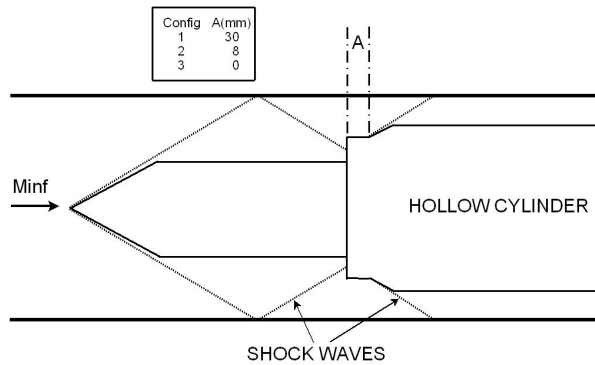

Figure 1: Two-shock experimental model (not to scale).

Computational Fluid Dynamics Program

Experimental Model CFD Design

The commercial code CFD-Fastran produced by ESI Software was used to model the flow as described in the experimental program. This program uses a compressible flow, finite volume, Navier-Stokes solver. The current simulations have been done with ideal gas and both Baldwin and Lomax and $k - \omega$ turbulence models. Ideal gas was used due the low enthalpy of the flow with expected maximum temperatures in the model well below 800K at which we would expect vibrational modes to cause thermal effects[4]. In Fastran, the experimental model was constructed as an axisymmetric model (Fig. 2) with clustering of cells on the duct inner wall where the shock wave/turbluent boundary layer interactions occur. The CFD model was grid refined to give a clear indication of grid independence. The duct inlet conditions were input as those at the exit of the shock tube nozzle i.e. $u = 1700m/s, v = 0m/s, w = 0m/s, P = 2100Pa, T = 100K$. All walls were modeled as isothermal with $T = 300K$, outlets were extrapolated meaning that all flow variables are extrapolated to the exit boundary from the domain interior, and the initial conditions were set as those of the experimental dump tank before firing namely $p = 133Pa, T = 300K$ and a small velocity along the centreline axis of $10m/s$ to prevent the initial calculation from failing.

The heat flux parameter q_w (Eq. 1) in CFD-View (ESI Software's post-processor software) was used to calculate the heat flux near the wall. Since the walls were modeled as isother-

mal the heat data was extracted from the cell next to the wall. The temperature gradient was determined to be closely linear so there was no need for manipulation of the heat flux equation for the proposes of this study.

$$q_w = \kappa \frac{T_c - T_w}{\delta} \qquad (1)$$

where κ is the thermal conductivity, δ is the projected distance from the wall face centroid to the cell centroid, T_c is the cell centre temperature and T_w is the wall temperature.
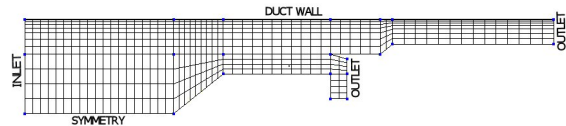

Figure 2: Sample CFD grid construction (not to scale and actual grid resolution not able to be shown).

Proposed Model CFD Design

In order to produce a stronger second shock interaction and therefore cause boundary layer separation, greater compression was required. This necessitated removing the radial outlet as used on the existing experimental model and replacing it with an outlet to swallow the first reflected shock that was axial (Fig. 3). This allowed room for the second cone base radius to be increased to provide sufficient compression and still be within the confines of the existing 38mm diameter duct.

The proposed model grid has been created in a very similar manner to the existing model grid with cell clustering at the duct inner wall. The Baldwin and Lomax and $k - \omega$ turbulence models have both been applied to allow comparison of separation results. The Baldwin and Lomax model should behave poorly as compared to the $k - \omega$ model because it is devoid of any information about the flow history[1]. Also the Boussinesq approximation and 'equilibrium' approximations implicit in algebraic models can not provide accurate calculation of separated flows[1].
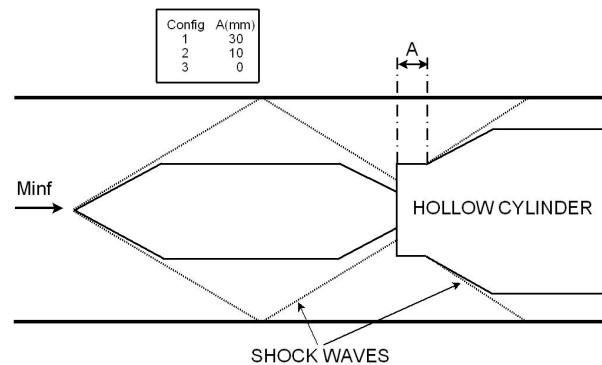

Figure 3: Proposed two-shock experimental model (not to scale).

Results and Discussion

Existing Model CFD Results

The comparison of experimental and computational results for each experimental configuration can be seen in Fig.s 4, 5 and 6 for pressure and Figs.7, 8 and 9 for heat flux. In each figure an approximate representation of the experimental model has been placed at the top to allow expected interaction location and data comparison. The figures show generally excellent agreement of experimental and computational results as follows.

In Configuration 1 (Fig. 4), the Baldwin and Lomax and $k - \omega$ turbulence models show excellent agreement with the experimental results for the pressure ratios. When comparing the heat flux (Fig. 7), the Baldwin and Lomax model is also in excellent agreement however the $k - \omega$ model over-predicts the heat flux significantly, over twice the value at the first interaction and over a half the value at the second interaction. The interaction positions axially are very well predicted and the viscous interaction off the leading edge of the hollow cylinder is also seen computationally.

In Configuration 2 (Fig. 5), the Baldwin and Lomax and $k - \omega$ turbulence models show excellent agreement with the experimental results for the pressure ratios. The Baldwin and Lomax model is also in excellent agreement when compared with the heat flux data (Fig. 8) however the $k - \omega$ model over-predicts the heat flux significantly once again, over twice the value for both interaction peaks. The first interaction position is not as well predicted for both turbulence models as it was in Configuration 1 but the second interaction is very well predicted as are the subsequent reflected shocks downstream of the second interaction.

The final configuration, Configuration 3, shows the greatest variation of experimental and computational data. The Baldwin and Lomax model still gives excellent prediction of the peak pressure and interaction locations for both interactions (Fig. 6). The $k - \omega$ turbulence model over-predicts the peak pressure for the second interaction by almost 100% but is in excellent agreement for the first interaction and the reflected shocks downstream of the second interaction. The peak heat flux locations (Fig. 9) are well predicted by both models however the Baldwin and Lomax model under-predicts the second interaction peak and the $k - \omega$ turbulence model over-predicts the first and second interaction heat fluxes by approximately a half and one and a half respectively.
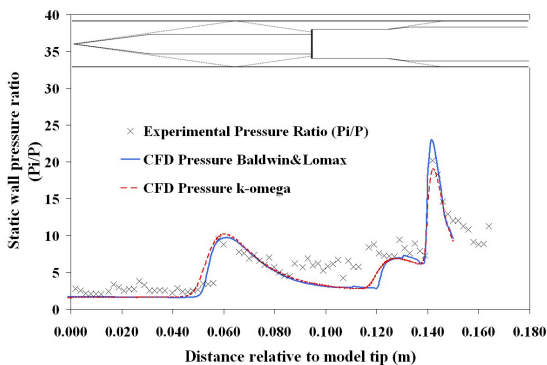

Figure 4: Comparison of pressure data for experimental and CFD results for configuration 1.

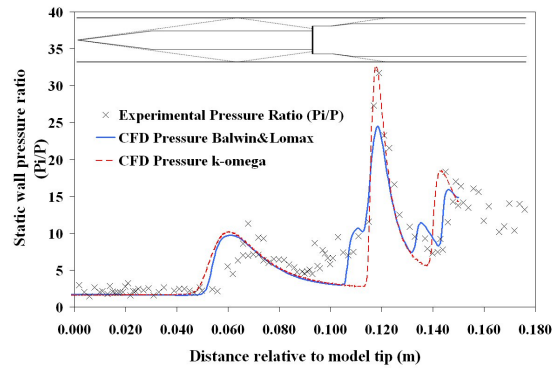The Baldwin and Lomax turbulence model has more accurately

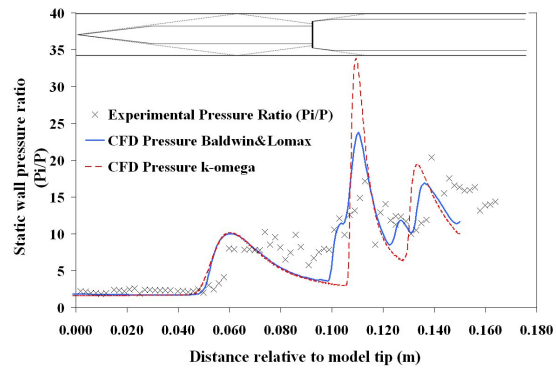Figure 5: Comparison of pressure data for experimental and CFD results for configuration 2.

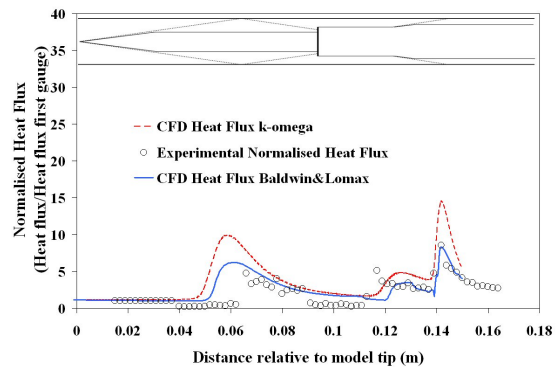Figure 6: Comparison of pressure data for experimental and CFD results for configuration 3.

Figure 7: Comparison of heat flux data for experimental and CFD results for configuration 1.

modeled the pressure and heat flux ratios as compared to the experimental data for three experimental configurations. It has more successfully captured the peak pressures and heat fluxes in this unseparated flow. The $k - \omega$ model has over-predicted pressure and heat flux ratios and this is partially due to the absence of a stress limiter which is not available on this version of the model (Wilcox 1991). The stress limiter serves to limit the
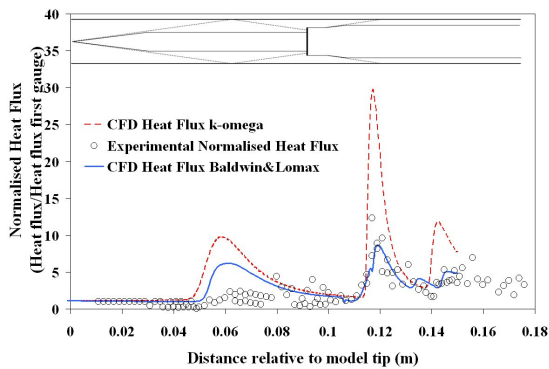
Figure 8: Comparison of heat flux data for experimental and CFD results for configuration 2.
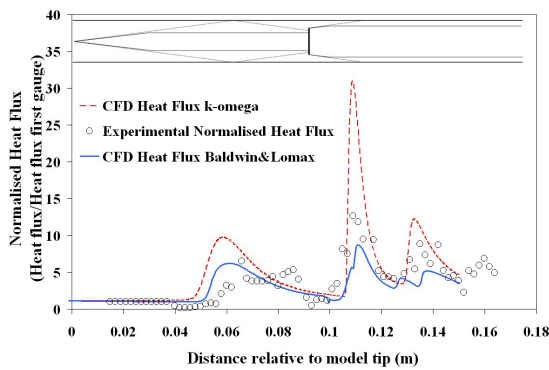

Figure 9: Comparison of heat flux data for experimental and CFD results for configuration 3.

kinematic eddy viscosity when energy production due to turbulence exceeds its dissipation[1].

Proposed Model CFD Results

A series of simulations with increasing second cone base radius (or increasing mass flow rate compression ratio) were performed using both Baldwin and Lomax and $k-\omega$ turbulence models. The results of these simulations are summarised in Fig. 10 which plots increasing mass flow rate compression ratio against the static wall pressure ratio. When the mass flow rate compression ratio reaches approximately 2.78 the $k-\omega$ model predicts no further increase in pressure ratio. There is a sudden rise in pressure ratio when the Baldwin and Lomax model reaches a mass flow rate compression ratio of approximately 3. The simulations above 3.05 mass flow rate compression ratio for the Baldwin and Lomax model became unsteady due to choking of the duct. The region from $2.78-3.05$ mass flow rate compression ratio is the most interesting area and may be indicative of an incipient to full separation region. This amount of mass flow rate compression (approximately $13.5-14.1mm$ second cone base radius) will therefore be targeted in the design of the proposed model.

Since the proposed model has compressed the flow more that the existing model, velocity profiles of the final section of the duct were examined to determine that distinct boundary layers were present on the upper and lower walls. Figure 11 shows the
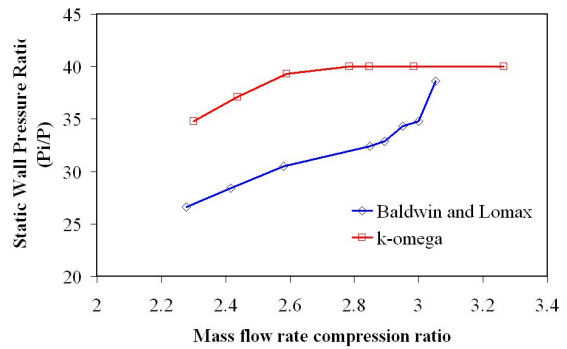

Figure 10: Turbulence model compression investigation for proposed two-shock model.

velocity profiles for the Baldwin and Lomax and $k-\omega$ turbulence models with 2.85 mass flow rate compression ratio. The flat regions between each curved profile near the walls indicate separate boundary layers. It is evident that a region of uniform freesteam still exists between the boundary layers and it is not full developed pipe flow.

Pressure contour plots were used to observe shock positions including the swallowing of the first reflected shock. Also reverse flow can be shown by plotting velocity vectors on these contour plots. Figure 12 shows a typical pressure contour plot of the rear half of the duct with the Baldwin and Lomax model. The circled region just ahead of the second shock wave/boundary layer interaction is indicative of a separation bubble. All simulations using the Baldwin and Lomax model above the 2.28 mass flow rate compression ratio point exhibit this separation region which was not observed experimentally at the same peak pressures.
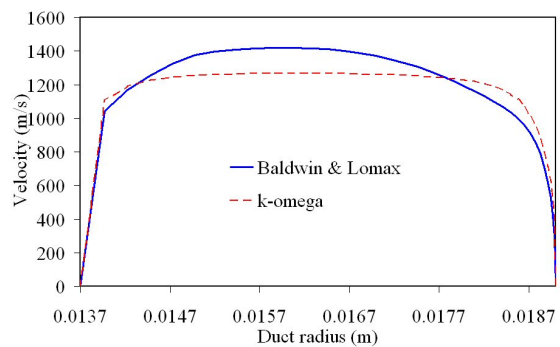

Figure 11: Velocity profiles across rear of duct for proposed two-shock model.
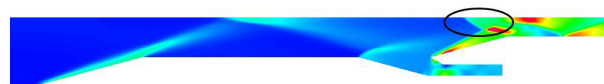

Figure 12: Pressure contours from CFD-Fastran in proposed two-shock model.

Typical computational results for the proposed model with a mass flow rate compression ratio of 2.85 (or second cone base

radius of 13.7mm) can be seen in Fig.s 13 and 14. As with the other figures, an approximate representation of the experimental model has been placed at the top to allow expected interaction location and data comparison. These figures show significant differences between the two turbulence models. For the pressure ratios, both models have a similar trend except that the Baldwin and Lomax model predicts separation at the second shock wave/boundary layer interaction point as evidenced by the inflection at approximately 0.125m. The velocity vectors at this point show a reverse velocity region as would be expected. The $k-\omega$ model predicts a peak pressure ratio that should cause separation according to the incipient separation correlations of Korkegi[5] yet the Baldwin and Lomax model peak pressure is not high enough according to the same correlations despite the separation inflection point noted.

The heat flux ratios are also significantly different. The $k-\omega$ model predicts a peak heat flux at the second interaction which is 2.5 times that of the Baldwin and Lomax model. This is consistent with the $k-\omega$ model heat flux calculations of the existing experimental model. Once again the most probable reason why the $k-\omega$ model over-predicts the peak heat flux and to some degree the peak pressure, is that this version of the model does not include a stress limiter. In the experimental data and Baldwin and Lomax model predictions, the Baldwin and Lomax model consistently under-predicts the peak heat flux. We might therefore reasonably conclude that the actual heat flux will fall between the predictions of these two turbulence models.
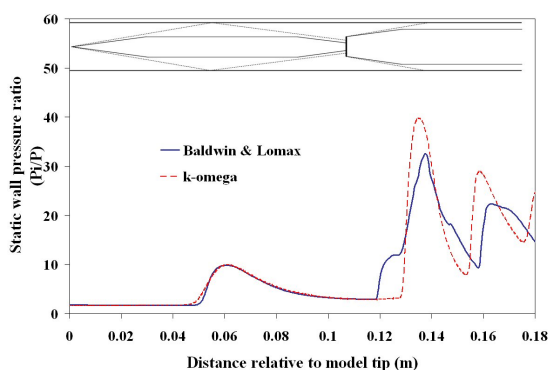

Figure 13: Pressure ratios determined by Baldwin and Lomax and $k-\omega$ turbulence models in proposed two-shock model with second cone base radius of 13.7mm.

Conclusions

CFD-Fastran has been used to model shock wave/boundary layer interactions in hypersonic flows. The software was used to replicate conditions and geometry of a model which has been previously tested and also to predict flow through a new model designed to produce separation of the boundary layer. In the experimental model, a turbulent boundary layer was subjected to two quantified compression-expansion systems, with an adjustable axial separation between them. CFD-Fastran has been successful in demonstrating that it is characterising the flow correctly for the existing experimental model. The Baldwin and Lomax turbulence model has been more successful than the $k-\omega$ turbulence model at predicting these unseparated flows. Both turbulence models have been applied to design an experimental model which will induce separation. The $k-\omega$ turbulence model simulations did not predict any boundary layer separation despite predicting pressure ratios that should cause separation. The Baldwin and Lomax turbulence model predicted
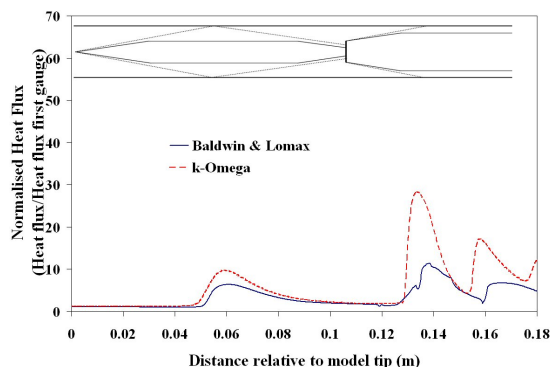

Figure 14: Heat flux ratios determined by Baldwin and Lomax and $k-\omega$ turbulence models in proposed two-shock model with second cone base radius of 13.7mm.

separation at all mass flow rate compression ratios above 2.28 which was not observed in the experimental data. Hence the design of the new model will incorporate a compromise of the two turbulence model results and the data will be useful for clarifying an area of theoretical uncertainty.

References

[1] Wilcox, D. C., *Turbulence modeling for CFD*, Third Ed., DCW Industries, La Canada, California, 2006.

[2] Dann A. G., Denman A. W., Jacobs P. A., Morgan R. G.: Study of separating compressible turbulent boundary-layers, AIAA Paper 2006-7943, 2006.

[3] Morgan R. G., Stalker R. J., Shock Tunnel Measurements of Heat Transfer in a Model Scramjet, *AIAA paper 85-908*, 1985.

[4] Anderson, J. D., *Hypersonic and High Temperature Gas Dynamics*, AIAA, Reston, Virginia, 2000.

[5] Korkegi R. H., Comparison of shock-induced two- and three-dimensional incipient turbulent separation, *AIAA Journal*, 13(4):534-535, Apr. 1975.